

TRANSVERSE DECOHERENCE OF ION BUNCHES WITH SPACE CHARGE AND FEEDBACK SYSTEM

I. Karpov¹, V. Kornilov², O. Boine-Frankenheim^{1,2}

¹TEMF, TU Darmstadt, Schloßgartenstraße 8, 64289 Darmstadt, Germany

²GSI, Planckstr. 1, 64291 Darmstadt, Germany

Abstract

The transverse decoherence of the bunch signal after an initial bunch displacement is an important process in synchrotrons and storage rings. It can be useful, for the diagnostic purposes, or undesirable. Collective bunch oscillations can appear after the bunch-to-bucket transfer between synchrotrons and can lead to the emittance blow-up. In order to preserve the beam quality and to control the emittance blow-up, transverse feedback system (TFS) are used. In heavy ion and proton beams, like in SIS18 and SIS100 synchrotrons of the FAIR project, transverse space charge strongly modify decoherence. The resulting bunch decoherence and beam blow-up is due to a combination of the lattice settings (like chromaticity), nonlinearities (residual or imposed by octupole magnets), strong space-charge, and the TFS. We study these effects using particle tracking simulations with the objective of correct combinations for a controlled beam blow-up.

DECOHERENCE DUE TO TRANSVERSE NONLINEARITY AND CHROMATICITY

A beam after an initial transverse displacement performs betatron oscillations. In the absence of collective effects, the evolution of the beam centroid has been described in [1, 2]. Calculations are performed for the case of transverse nonlinearity in one plane, the initial Gaussian distribution (GS) in (x, x') , the linear synchrotron motion and the Gaussian energy distribution. Extension to 2-D, including $x-y$ coupling in the tune dependence from amplitudes, is addressed in [3]. Here we present the 1D results for the KV (Kapchinsky-Vladimirsky) distribution in the transverse plane in the case of uncoupled transverse oscillations and compare with the results for the GS distribution and with particle tracking simulations.

We use the constant focusing for derivations and for simulations. In this case it is convenient to use the normalized coordinates,

$$q = \frac{x}{\sigma_{x0}} \text{ and } p = \frac{Rx'}{Q_0\sigma_{x0}}, \quad (1)$$

where R is the ring radius, Q_0 is the bare tune, $\sigma_{x0} = \sqrt{R\epsilon_{rms0}/Q_0}$ is the initial rms beam size, ϵ_{rms0} is the initial rms emittance. We normalize the initial beam offset in x plane by defining $Z = \Delta x/\sigma_{x0}$. The amplitude a and the phase ϕ of single particle oscillations are defined by relations $q = a \cos(\phi)$ and $p = -a \sin(\phi)$, where $a = \sqrt{q^2 + p^2}$.

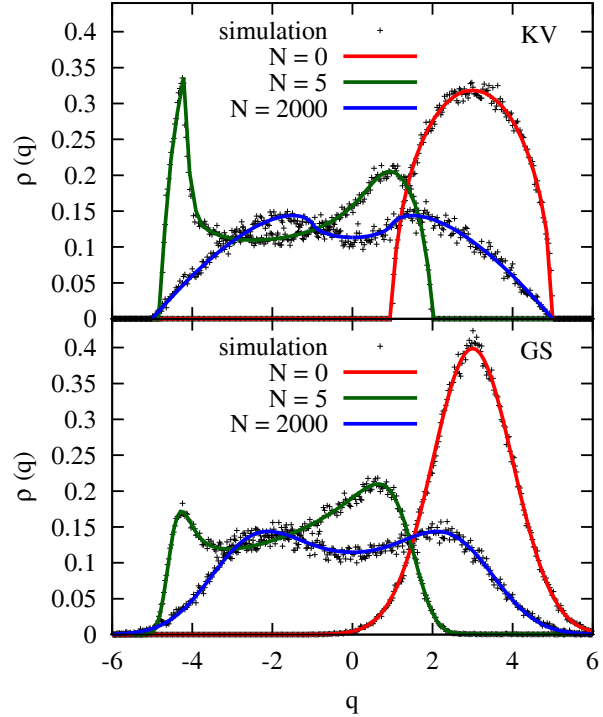


Figure 1: Beam profiles at different turn numbers for the KV (top plot) and for the GS (bottom plot) distributions. Crosses are simulation results. Solid lines are obtained by the numerical integration of Eq. (7). $Z = 3$, $Q_0 = 4.18$, $q_{nl} = 0.3$.

The initial beam distribution at turn $N = 0$ is

$$\rho_0(a, \phi_0) = \frac{a}{4\pi} H \left[1 - \frac{1}{4} (a^2 + Z^2 - 2aZ \cos(\phi_0)) \right], \quad (2)$$

where H is the Heaviside function and ϕ_0 is the initial betatron phase of the particle. External nonlinearities induce amplitude-dependent incoherent tune shifts. We assume that a transverse nonlinearity is produced by the cubic component of the octupole magnetic field,

$$B_x = -K_3 \frac{B\rho}{6} y^3, \quad B_y = K_3 \frac{B\rho}{6} x^3, \quad (3)$$

with $K_3 = \frac{1}{B\rho} \frac{d^3 B_y}{dx^3}$.

The resulting tune shift in x plane is given by

$$\Delta Q_{nl}(a) = -\frac{K_3 R^3}{16 Q_0^2} \epsilon_{rms0} a^2 = -\mu a^2, \quad (4)$$

where μ is the lattice detuning. The parameter for the effect of transverse nonlinearity is defined as a ratio of the nonlinearity tune shift Eq. (4) of a particle with the amplitude $a = 2$ to to the synchrotron tune Q_s ,

$$q_{nl} = \frac{4\mu}{Q_s}. \quad (5)$$

For single particle motion the amplitude a stays constant and the phase changes as

$$\phi = \phi_0 + 2\pi N(Q_0 - \mu a^2) = \phi_0 + \Delta\phi_N. \quad (6)$$

This allows us to get the particle distribution at arbitrary turn number N with substitution of ϕ_0 by $(\phi - \Delta\phi_N)$ in Eq. (2). Using Eqs. (2) and (6) a beam profile can be calculated as

$$\rho(q) = \frac{1}{4\pi} \int dp H \left[1 - \frac{1}{4} (q - Z \cos(\Delta\phi_N))^2 - \frac{1}{4} (p - Z \sin(\Delta\phi_N))^2 \right]. \quad (7)$$

and Figure 1 demonstrates a comparison of the beam profiles for the GS and the KV distributions at different turn numbers. $N = 2000$ corresponds to complete filamentation of the initial distribution due to transverse nonlinearities.

In the case of the linear synchrotron oscillation the tune shift due to chromaticity is defined as

$$\Delta Q_\xi = \xi Q_0 \delta \quad (8)$$

where ξ is the normalized chromaticity and $\delta = \Delta p/p_0$ is the relative momentum offset of the particle.

Similar to [1, 2] we calculate time evolution of the beam centroid. The amplitude is

$$A_{KV} = \sqrt{\langle q^2 \rangle + \langle p^2 \rangle} = \frac{J_1(2Z\theta)}{\theta} F_\xi, \quad (9)$$

and the phase is

$$\psi = 2\pi N (Q_0 - \mu(4 + Z^2)), \quad (10)$$

where J_n is the Bessel function of the first kind of the n th order, $\theta = 4\pi\mu N$ is the normalized time and the chromatic factor F_ξ ,

$$F_\xi = \exp \left[-2 \left(\frac{\xi Q_0 \sigma_\delta}{Q_s} \right)^2 \sin^2(\pi Q_s N) \right], \quad (11)$$

which provides an additional modulation due to the synchrotron motion with the tune Q_s [1], where σ_δ is the normalized rms momentum spread.

For comparison, the amplitude evolution for the initial GS distribution is given by [2]

$$A_{GS} = \frac{ZF_\xi}{1 + \theta^2} \exp \left[-\frac{Z^2\theta^2}{2(1 + \theta^2)} \right]. \quad (12)$$

The second momenta are given by

$$\begin{bmatrix} \langle q^2 \rangle \\ \langle qp \rangle \\ \langle p^2 \rangle \end{bmatrix} = \begin{pmatrix} 1 + \frac{Z^2}{2} \\ 0 \\ 1 \end{pmatrix} + \frac{ZF_\xi^2 J_1(4Z\theta)}{4\theta} \begin{bmatrix} \cos(2\psi) \\ -\sin(2\psi) \\ -\cos(2\psi) \end{bmatrix}$$

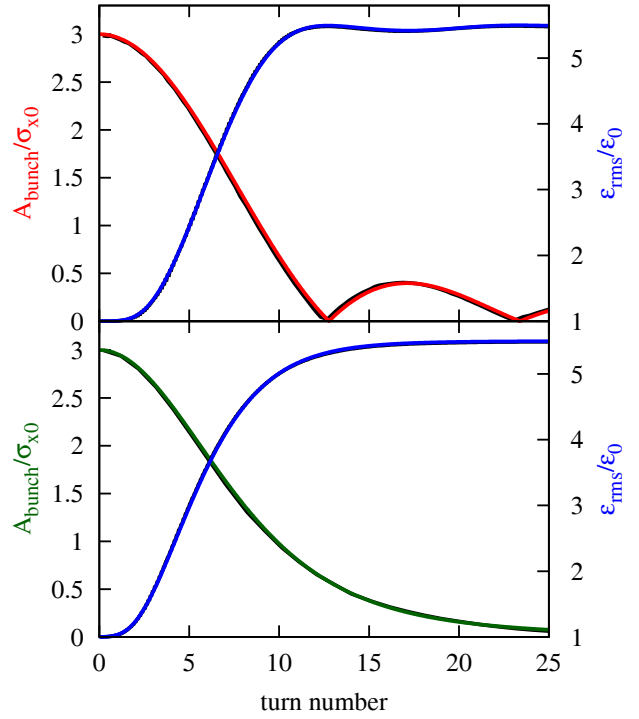


Figure 2: Time evolution of the beam offset amplitude and of the rms emittance for the KV (top plot) and for the GS (bottom plot) distributions. Black curves are simulation results, red curves are given by Eq. (9), green curves are given by Eq. (12) and blue curves are given by Eq. (14). $Z = 3$, $Q_0 = 4.18$, $q_{nl} = 0.3$.

$$+ \frac{F_\xi^2 J_2(4Z\theta)}{2\theta} \begin{bmatrix} \sin(2\psi) \\ -\cos(2\psi) \\ -\sin(2\psi) \end{bmatrix} \quad (13)$$

Using Equations (9, 10, 13) we calculate the normalized rms beam size and the normalized rms emittance as $\sigma_q = \sqrt{\langle q^2 \rangle - \langle q \rangle^2}$ and

$$\epsilon_{rms} = \epsilon_{rms0} \sqrt{\sigma_q^2 \sigma_p^2 - (\langle qp \rangle - \langle q \rangle \langle p \rangle)^2} \quad (14)$$

correspondingly. Figure 2 shows a comparison of the offset amplitude A_{bunch} and the rms emittance from particle tracking simulations for both distributions of the same initial rms size with Eqs. (9, 12, 14). According to Eq. (14), the final emittance does not depend on the initial distribution and for $N \rightarrow \infty$ we have

$$\epsilon_{rms} = \epsilon_{rms0} (1 + Z^2/2) \quad (15)$$

DECOHERENCE WITH SPACE CHARGE

The particle tracking code PATRIC [4] is used to study to damping of coherent oscillations and emittance blow-up due to decoherence with space charge [5]. As have been shown in Fig. 1 the beam profile significantly changes from the initial shape during the filamentation process. It requires to use a 2.5D self-consistent space charge solver in simulations.

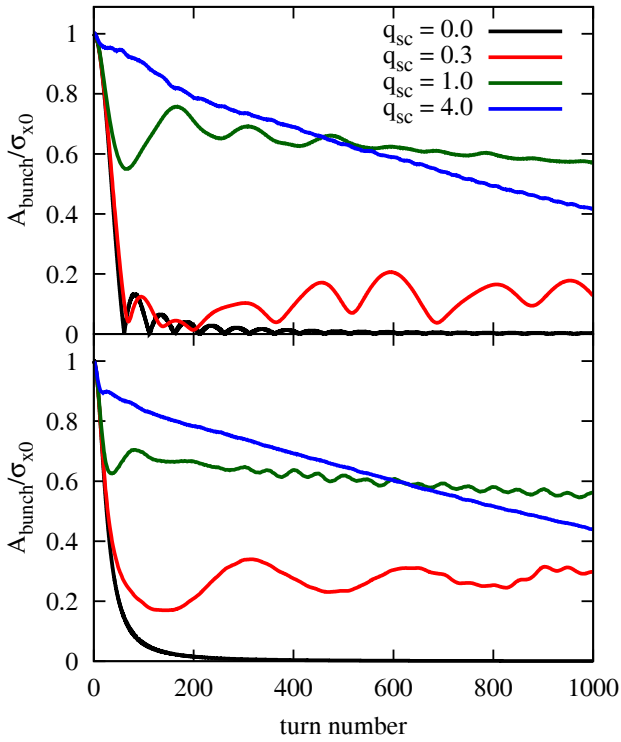


Figure 3: Time evolution of the bunch offset amplitude for the KV (top plot) and for the GS (bottom plot) distributions for $q_{nl} = 1$.

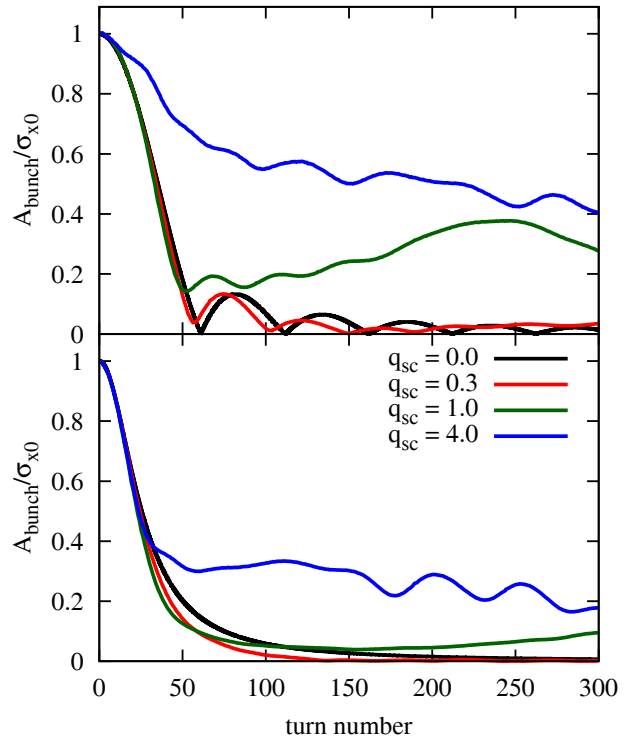


Figure 5: Time evolution of the bunch offset amplitude for the KV (top plot) and for the GS (bottom plot) distributions for $q_{nl} = -1$.

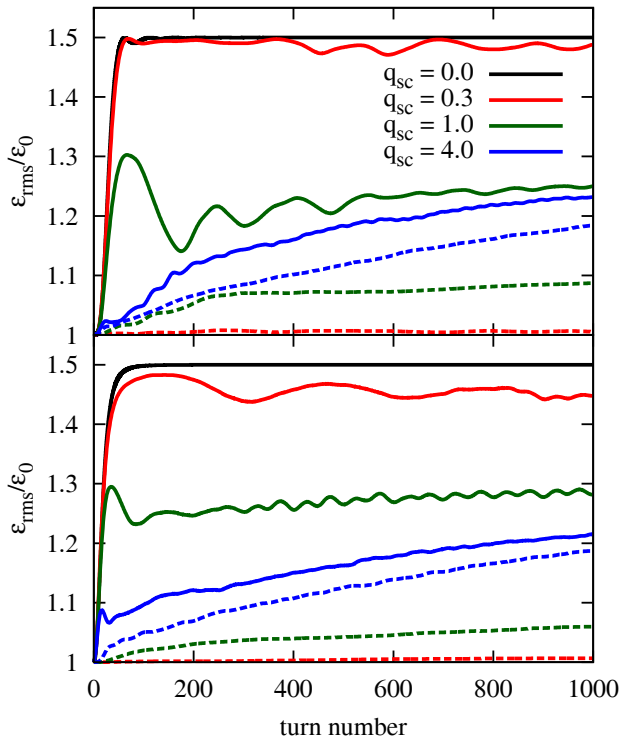


Figure 4: Time evolution of the rms emittance for the KV (top plot) and for the GS (bottom plot) distributions for $q_{nl} = 1$. Solid lines are ϵ_x , dashed lines are ϵ_y .

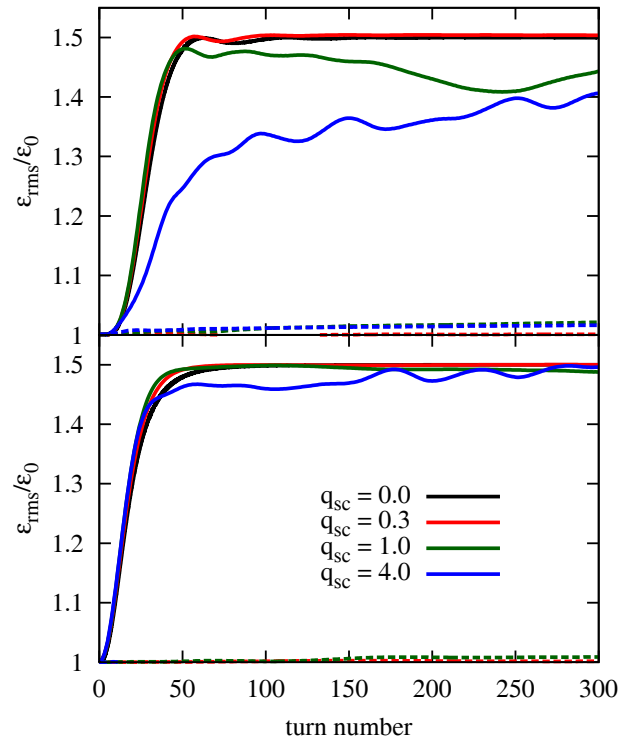


Figure 6: Time evolution of the rms emittance for the KV (top plot) and for the GS (bottom plot) distributions for $q_{nl} = -1$. Solid lines are ϵ_x , dashed lines are ϵ_y .

Transverse space charge effects are described using the characteristic tune shift,

$$\Delta Q_{sc} = \frac{\lambda_0 r_p R}{\gamma^3 \beta^2 \epsilon_{\perp}} \quad (16)$$

where β and γ are the relativistic parameters, $r_p = q_{ion}^2 / 4\pi\epsilon_0 mc^2$ is the classical particle radius, λ_0 is the peak line density (at the bunch center), and ϵ_{\perp} is the transverse total emittance. The tune shift corresponds to a round cross section with the KV distribution, and is defined as the modulus of the negative shift. In the rms-equivalent bunch with the GS transverse profile, i.e., the transverse rms emittance is $\epsilon_{rms} = \epsilon_{\perp}/4$, the maximum space charge tune shift is twice this value, $\Delta Q_{sc}^{max} = 2\Delta Q_{sc}$. The parameter for the effect of space charge in a bunch is defined as a ratio of the characteristic tune shift Eq. (16) to the synchrotron tune,

$$q_{sc} = \frac{\Delta Q_{sc}}{Q_s}. \quad (17)$$

All simulations below are performed for $Q_s = 0.01$, $Q_0 = 4.18$, $Z = 1$ and $\xi = 0$. Figures 3 and 4 demonstrate particle tracking simulations for an initially offset bunch with a round cross section for the KV (top plots) and the GS (bottom plots) distributions, for $q_{nl} = 1$. For $q_{sc} = 0$ (black lines) in Fig. 3 we see fast decrease of the bunch offset amplitude, as expected from Eqs. (9, 12), but for $q_{sc} = 0.3$ the bunch offset oscillations are not finally damped. For stronger space charge initial behavior of the bunch offset corresponds to Eqs. (9, 12) and then it changes to a different damping regime. In Fig. 4 one can see that the rms emittance approaches the asymptotic value (Eq. 15) only for $q_{sc} = 0$ and for $q_{sc} = 0.3$ in a bunch with the initial KV distribution. Note a slow emittance increase in both transverse planes for $q_{sc} > 1$. According to simulations, the emittance blow-up for both initial distributions is comparable.

In Figures 5 and 6 we show particle tracking simulations for the same bunch parameters in case of opposite polarity of transverse nonlinearity $q_{nl} = -1$ for the KV (top plots) and the GS (bottom plots) distributions. Damping of coherent

oscillations is faster for both distributions in comparison to the case of $q_{nl} = 1$ (Fig. 3). The final emittance in x plane for the GS distribution reaches the asymptotic value (Eq. 15) for all cases and is negligible in y plane. In the case of moderate and strong space charge for the KV distribution we observe the smaller emittance increase in x plane than for the GS distribution.

As we can see the damping process extremely depends on the sign of the transverse nonlinearity tune shift in the case of moderate and strong space charge. Figure 7 demonstrates comparison of the final particle distribution in a normalized phase space for $q_{nl} = 1$ and $q_{nl} = -1$ with the initial KV distribution. Strong space charge ($q_{sc} = 4$) in combination with nonlinearity polarity provides different redistribution of particles in the phase space and different emittance increase. To understand these effects an additional study is required.

TRANSVERSE FEEDBACK SYSTEM VS DECOHERENCE

In our simulations we use a simplified transverse feedback system (TFS) module with two elements: a beam position monitor (BPM) which measures the bunch offset and combines values from two turns to provide the correctional signal Δp_N with the required phase for the kicker. For the constant focusing lattice the correctional signal is given by

$$\Delta p_N = G q_N \frac{\cos(\Delta\phi + 2\pi Q_0)}{\sin(2\pi Q_0)} - G q_{N-1} \frac{\cos(\Delta\phi + 4\pi Q_0)}{\sin(2\pi Q_0)}, \quad (18)$$

where $\Delta\phi$ is the phase advance between the BPM and the kicker, G is the TFS gain which defines the damping time,

$$N_{TFS} = \frac{2}{G}. \quad (19)$$

In this model we assume that the TFS module has no bandwidth limitations, delay errors and noise amplification. In order to prevent emittance blow-up the damping time

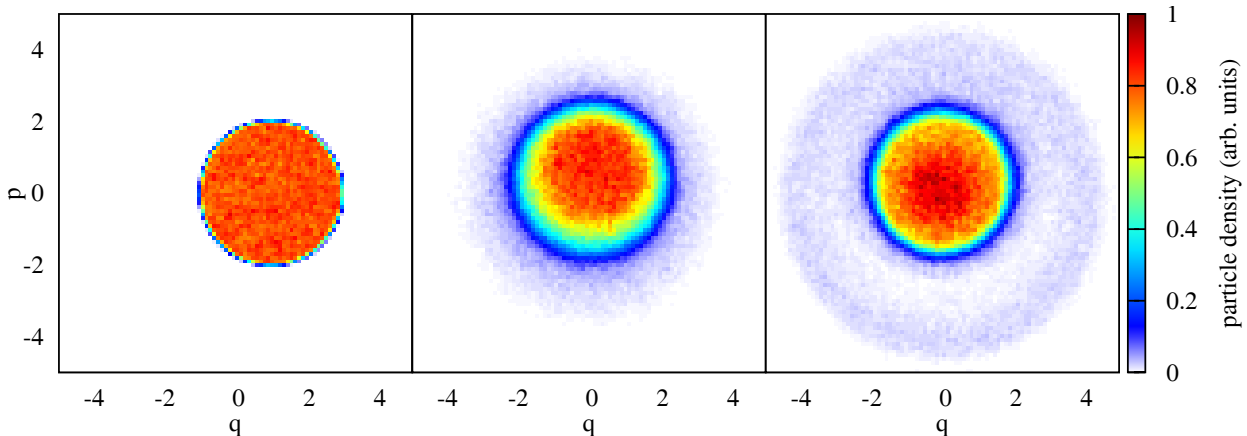


Figure 7: A particle density in the normalized phase space (p, q) for the initial KV distribution at $N = 0$ (left plot), $N = 1000$ $q_{nl} = 1$ (center plot) and $N = 1000$ $q_{nl} = -1$ (right plot), $q_{sc} = 4$.

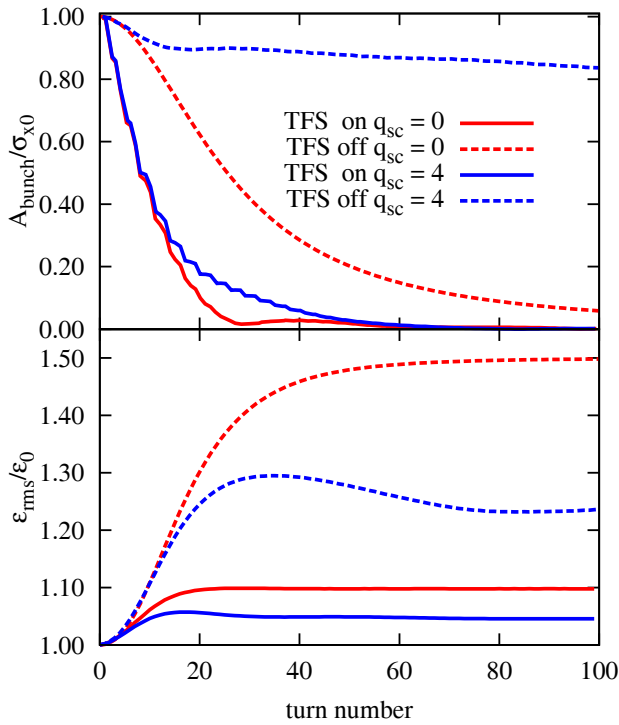


Figure 8: Time evolution of the bunch offset amplitude (top plot) and the rms emittance (bottom plot) for the initial GS distribution with TFS (solid lines) and without TFS (dashed lines). The parameters of simulations: $q_{nl} = 1$, $q_{sc} = 0; 4$, $N_{\text{TFS}} = 10$, $\Delta\phi = \pi/8$.

N_{TFS} should be smaller than characteristic decoherence time. Figure 8 shows an example of particle tracking simulations of an initially offset bunch with a round cross section for the GS distribution, for $Z = 1$, $q_{nl} = 1$ and the TFS damping time $N_{\text{TFS}} = 10$ turns. For comparison dashed lines correspond to simulations without TFS. We see that a simplified TFS module can considerably reduce the emittance blow-up due to transverse nonlinearity and space charge. The emittance increase with TFS in y plane is smaller than 1% and is not shown. One can also see that space charge could be helpful for emittance preservation.

CONCLUSIONS

The analytical prediction of emittance blow-up due to bunch decoherence with transverse nonlinearities for the initial transverse Kapchinsky-Vladimirsky distribution has been derived and compared, with the case of the initial Gaussian distribution. The bunch offset decoherence and transverse emittance blow-up have been studied using the particle tracking code PATRIC for different space charge strength. The different damping regimes of coherent oscillations for positive and negative polarity of octupole nonlinearity have been observed. The emittance blow-up reduction using an ideal Transverse Feedback System module has been shown.

ACKNOWLEDGMENTS

We thank Shaukat Khan (TU Dortmund) for useful discussions.

REFERENCES

- [1] R.E. Miller, A.W. Chao, J.M. Peterson, S.G. Peggs, M. Furman, SSC Report SSC-N-360 (1987)
- [2] M.G. Minty, A.W. Chao, W.L. Spence, Proceedings of PAC95, Dallas, Texas, USA, p. 3037 (1995)
- [3] S.Y. Lee, SSC Report SSCL-N-749 (1991)
- [4] O. Boine-Frankenheim, V. Kornilov, Proc. of ICAP2006, Oct 2-6, Chamonix Mont-Blanc, (2006)
- [5] V. Kornilov, O. Boine-Frankenheim, Transverse decoherence and coherent spectra in long bunches with space charge Phys. Rev. ST Accel. Beams 15, 114201 (2012).